Available online at www.sciencedirect.com
SCIENCE DIRECT
Catalysis Today 99 (2005) 59–67
CATALYSIS TODAY
www.elsevier.com/locate/cattod

Mechanistic aspects of the oxidative dehydrogenation of propane over an alumina-supported $VCrMnWO_x$ mixed oxide catalyst

Evgueni V. Kondratenko*, Maymol Cherian, Manfred Baerns

Institute for Applied Chemistry Berlin-Adlershof, Richard-Willstätter-Str. 12, D-12489 Berlin, Germany

Available online 21 December 2004

Dedicated to Prof. Ferruccio Trifiro on the occasion of his 65th Birthday.

Abstract

Mechanistic and kinetic aspects of the catalytic oxidative dehydrogenation of propane (ODP) were studied within a wide range of temperatures (673–773 K), partial pressures of oxygen (0–20 kPa), propane (0–40 kPa) and propene (0–4 kPa) under both steady-state ambient-pressure and transient, vacuum conditions in the temporal analysis of products (TAP) reactor. A $Mn_{0.18}V_{0.3}Cr_{0.23}W_{0.26}O_x$–$Al_2O_3$ catalyst was identified as a selective catalyst for ODP by high-throughput experiments. For comprehensive catalyst characterization, XRD, BET, and in situ UV–visible techniques were applied. The results from transient experiments in combination with UV–visible tests reveal that selective and non-selective propane oxidation occurs on the same active surface sites, i.e., lattice oxygen. CO_x formation takes place almost exclusively via consecutive propene oxidation, which involves both lattice and adsorbed oxygen species, with the latter being active in CO formation. However, the adsorbed species play a minor role. CO_2 formation was found to increase in the presence of propene in the reaction feed. Optimized operating conditions for selective propane oxidation were derived and discussed based on the experimental observations with respect to the influence of temperature and partial pressures of O_2, C_3H_6 and C_3H_8 on the reaction. In co-feed mode with a propane to oxygen ratio of 2, optimal catalytic performance is achieved at low partial pressures of oxygen and high temperature. Propene selectivity can be also improved by carrying out the ODP reaction in a periodic mode; that is an alternate feed of propane and air.

Keywords: Oxidative dehydrogenation; Propane; Vanadia; Chromia; $MnVCrWO_x$–Al_2O_3; Transient experiments; TAP reactor

1. Introduction

During the last decade the selective oxidation of light alkanes to their olefins or to other products with higher values (aldehydes, ketones, carboxylic acids, epoxides, etc.) attracted both industrial and scientific attention with respect to the development of new economically viable processes [1–3]. The oxidative dehydrogenation of propane (ODP) to propene is an alternative route for the production of propene as compared to catalytic non-oxidative dehydrogenation of propane. Propene is a major feedstock for the manufacturing of various industrially important products (e.g. polypropylene, acrolein, acrylic acid). The exothermicity of the ODP reaction enables the reaction temperatures to be lower than those required for catalytic non-oxidative propane dehydrogenation. Numerous catalysts have been tested for the ODP reaction with vanadium-based materials being most active and selective [1,4,5]. Different properties of the solid materials such as reducibility, acidity and basicity, coordination geometry and dispersion of VO_x species have been identified as being important in affecting catalytic performance in oxidative dehydrogenation of light alkanes [6–11].

Since the desired products (olefins, oxygenates) of the selective conversion of light alkanes are usually more reactive than the respective alkanes, the main task for oxidative dehydrogenation (OHD) reactions is the minimization of the undesired side reactions resulting in CO_x formation. This results in the need to isolate the selective reaction products before side products are formed. The extent of kinetic isolation of the selective products depends on the relative rates of the formation of a specific selective product and its rates of further conversion to CO_x. Therefore,

* Corresponding author. Tel.: +49 30 63924448; fax: +49 30 63924454.
E-mail address: evgenii@aca-berlin.de (E.V. Kondratenko).

0920-5861/$ – see front matter © 2004 Elsevier B.V. All rights reserved.
doi:10.1016/j.cattod.2004.09.024

a better understanding of the mechanism of ODH is essential to explore means of optimizing this reaction. Although the physico-chemical properties of catalytic materials have been extensively studied, only a few studies aimed at understanding the mechanism and the reaction kinetics [12–18]. The kinetic studies of ODP performed by Creaser and Andersson over a V–Mg–O catalyst suggested that the reaction rate has a higher order dependency on propane partial pressure than on oxygen partial pressure [19,20]. Studies on the effect of the partial pressure of oxygen suggest that higher propene selectivity can be achieved by lowering the oxygen partial pressure [21]. In previous studies, CO_x was suggested to originate from both total propane and propene oxidation. From their kinetic isotopic studies Chen et al. [16] concluded that over a VO_x/ZrO_2 catalyst, CO_2 is formed by both primary and secondary combustions, whereas, CO is formed by the secondary oxidation of propene. With respect to oxygen species, total oxidation is proposed to occur at different surface sites than that of selective propane dehydrogenation or to involve distinct forms of reactive oxygen [14,22,23]. In spite of the many studies on physico-chemical characterization of catalytic materials, still a more comprehensive understanding is required on the relationships between mechanistic and kinetic aspects of the ODP reaction as well as catalytic performance and solid-material properties for further improvement of the catalytic materials or process operation.

Against this background the present study aimed at elucidating mechanistic aspects of the ODP reaction in a wide range of oxygen, propane and propene partial pressures as well as of temperatures over $Mn_{0.18}V_{0.3}Cr_{0.23}W_{0.26}O_x$–$Al_2O_3$ as catalytic material. This catalyst composition was chosen based on our previous combinatorial studies on the oxidative dehydrogenation of propane [24] and ethane [25]. The highest propene yield of ca. 14% at the degree of propane conversion of 26% was achieved over this catalytic material. To achieve the above aims, steady-state ambient pressure and transient experiments in the temporal analysis of products (TAP) reactor in high vacuum were carried out. Kinetic and mechanistic insights into the ODP reaction derived are discussed with results of catalyst characterization that is, its structural, redox properties as well as vanadia and chromia distribution.

2. Experimental

2.1. Catalyst preparation

The mixed oxide catalyst $Mn_{0.18}V_{0.3}Cr_{0.23}W_{0.26}O_x$ on Al_2O_3 was prepared by the following procedure. The required amounts of Mn, V, Cr, W and Al precursors, i.e. $Mn(NO_3)_2{\cdot}4H_2O$, NH_4VO_3, $Cr(NO_3)_3{\cdot}9H_2O$, $Al(NO_3)_3$, respectively, were dissolved in water. The ratio of $Mn_{0.18}V_{0.3}Cr_{0.23}W_{0.26}O_x$ to Al_2O_3 was ca. 5, i.e. 15 wt.% corresponds to the active components. The aqueous precursor solution was absorbed on an ash-less filter paper, which was dried at 393 K for 1 h and subjected to subsequent calcination at 973 K for 4 h according to a procedure described in [26].

2.2. Catalyst characterization

Catalytic specific surface area, vanadia and chromia distribution (isolated, polymerized species), reducibility, structure and phase composition of $Mn_{0.18}V_{0.3}Cr_{0.23}W_{0.26}O_x$–$Al_2O_3$ used as catalytic material were determined by using BET measurements, UV–visible diffuse reflectance, and, XRD spectroscopies, respectively. A short description of experimental details is given below.

The specific surface area was obtained by the single-point BET method (Gemini III analyzer) using physisorption of N_2 at 77 K.

For X-ray powder diffraction a STADIP transmission powder diffractometer (Stoe) with Cu $K\alpha_1$ radiation was used.

For UV–visible diffuse reflectance spectroscopy a Cary 400 Varian spectrometer was used which was equipped with a diffuse reflectance accessory (Prying mantis, Harrick). The catalyst sample was diluted with Al_2O_3 in a ratio of 1:10. The sample was preheated in a flowing O_2/N_2 mixture (O_2:N_2 = 1:9) at 773 K for ca. 30 min. The reduction of the sample was carried out with mixtures of hydrogen or propane in nitrogen (H_2:N_2 = 1:9, C_3H_8:N_2 = 1:9) at 773 K for 1 h and subsequently reoxidized in an O_2/N_2 flow (O_2:N_2 = 1:9) for 30 min. Two different reducing agents (H_2 and C_3H_8) were chosen in order to prove if the coke deposition takes place during reduction with propane.

The chemical composition of the catalyst sample was analyzed by inductively coupled plasma spectroscopy ICP-OES (Optima 3000XL, Perkin-Elmer).

2.3. Mechanistic studies in TAP reactor

Transient isotopic experiments were performed in order to derive insights into reaction pathways of propane dehydrogenation to propane as well as of propane/propene oxidation to CO_x. Particular attention was paid to understanding the role of lattice and adsorbed oxygen species in CO_x formation. For these purposes, the temporal analysis of products (TAP) microreactor made of quartz (40 mm long and 6 mm inner diameter) was used; the setup has been described in detail elsewhere [27,28]. The catalytic material (30 mg; d_p = 250–355 μm) was placed between two layers of quartz of the same particle size. Prior to each transient experiment, the catalyst was pretreated in an oxygen flow for 1 h at 773 K and ambient pressure. The pretreated catalyst was then exposed to vacuum (ca. 10^{-5} Pa) before the pulse experiments were carried out in a temperature range from 573 to 773 K. Different gas mixtures (C_3H_8:Ne = 1:1, C_3H_8:$^{18}O_2$:Ne = 2:1:2) were pulsed over the catalyst and the

transient responses were monitored at atomic mass units (AMU) related to the feed, reaction products and inert gas. One pulse consisted of 10^{14} to 5×10^{14} molecules. Pulses were repeated for each AMU 10 times and averaged to improve the signal-to-noise ratio. Ne (99.995), $^{18}O_2$ (95–98% of ^{18}O, ISOTEC), and C_3H_8 (99.95) were used without additional purification. The variations in feed components and reaction products were determined from the respective AMUs using standard fragmentation patterns and sensitivity factors.

2.4. Catalytic performance

For characterizing the performance of the catalytic material, tests were performed in an U-shaped fixed-bed reactor ($Ø_{i.d.}$ = 6 mm) made of quartz, at atmospheric pressure and different temperatures (673–773 K). The reactor was immersed into a bed of fluidized sand serving as a source or sink of heat. The temperature profile in the bed of catalyst particles was measured by an axially movable thermocouple inside a quartz-made capillary, placed in the bed. The highest hot-spot temperature was 15 K at a near to complete oxygen conversion using the most concentrated reaction mixture (C_3H_8:O_2:N_2 = 2:1:2). In other tests the temperature difference in the catalyst bed did not exceed 4 K. The experiments were performed with different feed compositions varying in the propane to oxygen ratio from 1:1 to 8:1. Partial pressures of propane were varied from 0.05 to 0.40 bars. In order to get additional insights into CO_x formation, steady-state experiments were carried with addition of propene to a C_3H_8/O_2 mixture (C_3H_8:O_2:Ne = 20:10:70). The homogeneous propane and propene oxidation was found to be negligible under the operating conditions. For catalyst particles of 250–350 μm, internal mass transfer is neglected. The absence of external mass-transfer limitations was proven by carrying out catalytic reaction at different flows, keeping constant residence time. Besides, the degrees of propane conversion is strongly increasing with temperature. This is not typical for reactions controlled by external mass transfer, since activation energy of gas-phase diffusion is ca. 10–20 kJ/mol. For acquiring selectivity data at different degrees of propane conversion the contact time was varied from 20 to 900 kg s m^{-3} by using different amounts of catalyst and total flow rates. The products and feed components were analyzed using online GC (HP 5890) equipped with Porapak Q and Molecular sieve-5 columns.

3. Results and discussion

The following three sections present and discuss the results of catalyst characterization, mechanistic and isotopic analysis of the ODP reaction in the TAP reactor and study the effects of reaction parameters such as O_2, C_3H_6 and C_3H_8 partial pressures as well as reaction temperature and contact time on the performance of the $Mn_{0.18}V_{0.3}Cr_{0.23}W_{0.26}O_x$–$Al_2O_3$ catalytic material in the ODP reaction. Afterwards reaction scheme of the ODP reaction is suggested, which explains the observed experimental phenomena. In conclusion, reaction operation conditions for achievement of high propene yield are suggested and discussed.

3.1. Surface and bulk compositions

The specific surface area of the catalyst amounted to ~195 m^2/g. No crystalline phases of the metal oxides were observed in the synthesized catalytic material. This is probably due to either very small crystalline domains (<40 nm), which are not detectable by XRD, or due to the existence of only amorphous phases.

The UV–visible spectra of the oxidized and reduced catalyst at 773 K are presented in Fig. 1. The data reveal the presence of monomeric and polymeric vanadia and chromia species. Charge-transfer (CT) bands were observed at 230, 251, 272 and 291 nm. The bands at 230 and 272 nm belong to isolated tetrahedrally co-ordinated V^{5+} species [29], while the bands at 251 and 291 nm are characteristic of tetrahedrally co-ordinated Cr^{6+} species [30]. Broad bands between 340 and 500 nm can be assigned to oligomeric vanadia or chromia species. It is difficult to separate vanadia and chromia species since both vanadia and chromia CT bands belong to a region of similar wavelength. CT bands due to manganese and tungsten oxides were not observed.

After reduction of $Mn_{0.18}V_{0.3}Cr_{0.23}W_{0.26}O_x$–$Al_2O_3$ by C_3H_8, the intensity of the CT bands between 230 and 300 nm

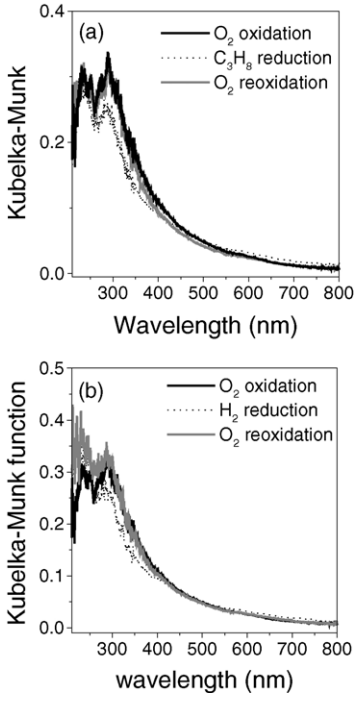

Fig. 1. UV–visible-DRS spectra of the $Mn_{0.18}V_{0.3}Cr_{0.23}W_{0.26}O_x$–$Al_2O_3$ catalyst after pretreatments at 773 K in: (a) C_3H_8:N_2 = 1:9 or O_2:N_2 = 1:4 mixtures; (b) H_2:N_2 = 1:9 or O_2/N_2 = 1:4 mixtures.

decreased significantly due to the reduction of V^{5+} and Cr^{6+} (Fig. 1a). The intensity of d–d transitions of V^{4+} species is several times lower than that of charge-transfer transitions of V^{5+} and Cr^{6+}, since the former transitions (V^{4+}) are forbidden. This result in difficulties for identification of d–d bands at relatively low degrees of catalyst reduction. However, an increase of the Kubelka-Munk function in the region from 500 to 800 nm, as shown in Fig. 1, can be ascribed to d–d transitions of V^{4+} and Cr^{3+} species. Remarkably, no additional bands appeared in the region of 300–600 nm; reflections in this region would have been characteristic for carbon deposition. A similar reduction behavior of V^{5+} and Cr^{6+} was also observed, when hydrogen was used as reducing agent (Fig. 1b). Based on these data it can be concluded that no significant carbon deposition occurs during catalyst reduction by propane. The reduced vanadium and chromium species are fully reoxidized by oxygen at the temperature of reduction as also shown in Fig. 1.

From these data, it can be concluded that $Mn_{0.18}V_{0.3}Cr_{0.23}W_{0.26}O_x$–$Al_2O_3$ oxidizes propane and hydrogen in the absence of gas-phase oxygen, i.e., lattice oxygen of the catalyst takes part at the reaction. Thus, for the present catalyst a Mars–Van Krevelen type reaction mechanism is expected [31]. In order to prove this suggestion, a detailed mechanistic analysis of the ODP reaction has been performed in the temporal analysis of products reactor using isotopically labeled molecules. The results are presented below.

3.2. Mechanistic insights into the ODP reaction from transient experiments in vacuum

On pulsing a mixture of propane and labeled oxygen ($^{18}O_2$) over the catalyst, which was preoxidized by $^{16}O_2$, CO_x products containing different oxygen isotopes (^{16}O and ^{18}O) were detected at the reactor outlet. The experimental data on the distribution of labeled oxygen in CO_x are presented in Fig. 2. The transient responses are presented in a normalized form for better comparison of the pulse shapes. CO and CO_2 contain both non-labeled (^{16}O) and labeled (^{18}O) oxygen. This indicates that there exist two independent reaction pathways with participation of labeled and non-labeled oxygen in CO_x formation. The distribution of labeled oxygen in CO_x is given in Table 1. It can be seen that $C^{16}O$ and $C^{16}O_2$ are the main CO_x products. This means that lattice oxygen of the catalyst is mainly responsible for CO_x formation. This is in agreement with the above-mentioned UV–visible results, which show the reduction of V^{5+} and Cr^{6+} species by propane (Fig. 1). It is important to note that the contribution of adsorbed oxygen species to CO formation is higher as compared to CO_2 formation (Table 1). Furthermore, adsorbed oxygen species formed from gas-phase labeled ($^{18}O_2$) oxygen play only a minor role. This may be due to the fact that the concentration of lattice non-labeled oxygen is considerably higher than that of pulsed labeled ($^{18}O_2$) gas-phase oxygen. The ratio of vanadium to the amount of oxygen in one pulse was estimated as ca. 5×10^3. Therefore, the role of adsorbed oxygen species may be underestimated under vacuum conditions. That is, at higher oxygen partial pressure, more adsorbed oxygen may exist. Based on these data, it can be anticipated that the reaction pathways of CO and CO_2 formation might differently depend on oxygen partial pressure, since concentration of adsorbed oxygen species is a function of oxygen partial pressure.

Table 1
Distribution of isotopically labeled oxygen in the yield of CO_x during pulsing a mixture of C_3H_8 and $^{18}O_2$ (C_3H_8:$^{18}O_2$:Ne = 2:1:2) over $Mn_{0.18}V_{0.3}Cr_{0.23}W_{0.26}O_x$–$Al_2O_3$ as catalyst at 773 K in the temporal analysis of products reactor (pulse size of Ne is ca. 2×10^{14} molecules)

$X(C_3H_8)$ (%)	30
$Y(C^{16}O)$ (%)	7.5
$Y(C^{18}O)$ (%)	1.6
$Y(C^{16}O_2)$ (%)	10.5
$Y(C^{16}O^{18}O)$ (%)	0.3

Pulsing of propane without gas-phase oxygen over the preoxidized catalyst, the amount of CO_x and propene formed changes with an increase in the amount of propane pulsed, which corresponds to the oxidation state of the catalyst. The results are presented in Fig. 3. The initial selectivity towards

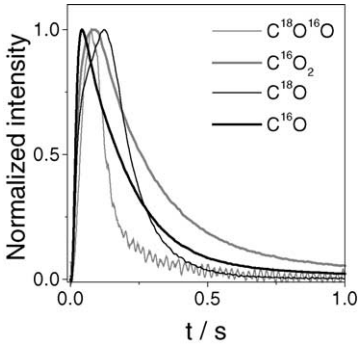

Fig. 2. Transient responses of carbon oxides formed on pulsing an $^{18}O_2$–C_3H_8 mixture (C_3H_8:$^{18}O_2$:Ne = 2:1:2) over the $Mn_{0.18}V_{0.3}Cr_{0.23}W_{0.26}O_x$–$Al_2O_3$ catalyst at 773 K.

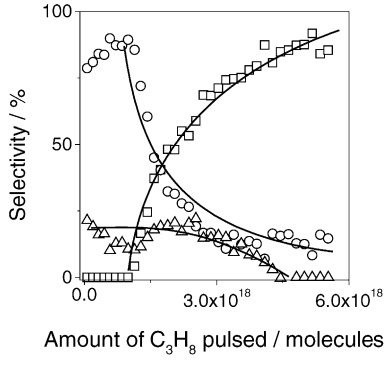

Fig. 3. Product selectivities in the ODP reaction as a function of the amount of propane pulsed over the $Mn_{0.18}V_{0.3}Cr_{0.23}W_{0.26}O_x$–$Al_2O_3$ catalyst at 773 K: (□) C_3H_6; (○) CO; (△) CO_2.

propene was very low at a degree of propane conversion of ca. 18%. However, the selectivity was improved with an increase in the amount of propane pulsed, while the degree of propane conversion did not strongly change. Similar results have been previously reported for the ODP reaction over VO_x/TiO_2 [13] and V–Mg–O [14] catalytic materials under transient oxygen-free conditions. A selectivity of nearly 100% to propene was achieved at ca. 15% degree of propane conversion. Since no gas-phase oxygen was pulsed with propane, the low initial selectivity towards propene is due to very high concentration of surface-lattice or strongly-adsorbed oxygen in comparison to the amount of propane within a single pulse. This results in a high initial propane conversion to propene followed by a fast secondary oxidation of the primarily formed propene to CO_x. With progressive propane pulsing the concentration of lattice oxygen decreases due to its removal by interaction with propane or propene. In this way active lattice oxygen becomes more isolated on the catalyst surface. In turn, the non-selective secondary oxidation of propene to CO_x is inhibited, since for CO_x formation more than one neighboring lattice oxygen species are needed. Thus, the degree of catalyst reduction is a key factor, which influences the selective route of ODP under transient conditions; from this result propene selectivity is expected to be affected by the oxygen partial pressure in a reaction mixture.

3.3. Influence of reactant partial pressures and temperature on steady-state oxidative propane dehydrogenation at ambient pressure

The ambient-pressure ODP reaction was studied at different temperatures and contact times using feed compositions with various oxygen and propane concentrations. For all feed compositions and reaction temperatures, C_3H_6, CO and CO_2 were the main reaction products. Small amounts of ethylene, methane and oxygenates (acrolein, acetaldehyde) were observed at high degrees of propane conversion. A typical relationship between product selectivities and the degrees of propane conversion is shown in Fig. 4. As expected, the propene selectivity decreases with

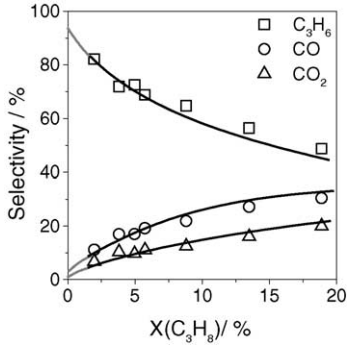

Fig. 4. Selectivity–conversion relationship of the ambient-pressure ODP reaction over $Mn_{0.18}V_{0.3}Cr_{0.23}W_{0.26}O_x$–$Al_2O_3$ at 773 K (C_3H_8:O_2:N_2 = 40:20:40).

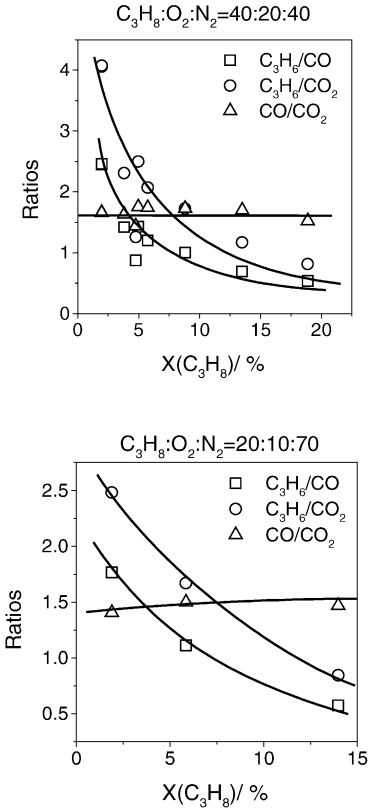

Fig. 5. Ratios of C_3H_6/CO, C_3H_6/CO_2 and CO/CO_2 vs. the degree of propane conversion over $Mn_{0.18}V_{0.3}Cr_{0.23}W_{0.26}O_x$–$Al_2O_3$ at 773 K.

an increase in propane conversion, while the selectivity towards CO and CO_2 increases correspondingly. From this dependence it is suggested that propene is formed directly from propane, while CO and CO_2 are mainly formed via secondary oxidation of propene. Direct propane oxidation to carbon oxides cannot fully be excluded. However, this reaction pathway should play a minor role in comparison to propene oxidation to CO_x. For identifying more precisely secondary reaction pathways, the ratios of C_3H_6/CO, CO/CO_2 and C_3H_6/CO_2 were plotted versus the degree of propane conversion for two different feed compositions (Fig. 5). As shown in these figures, the ratios of C_3H_6/CO and C_3H_6/CO_2 decrease with an increase in the degree of propane conversion. It also appears that the C_3H_6/CO_x ratios approach asymptotically very high values at very low degrees of propane conversion. However, the ratio of CO/CO_2 is relatively constant or slightly increases, i.e. secondary oxidation of CO to CO_2 can be excluded. Similar results were obtained for other reaction feeds and temperatures.

Table 2 shows catalytic performance of the $Mn_{0.18}V_{0.3}Cr_{0.23}W_{0.26}O_x$ on Al_2O_3 catalyst using a feed composition with 40 vol.% of propane, while the oxygen concentration was varied from 4 to 20 vol.%. For a clear presentation of the effect of oxygen partial pressure on products formation, the ratios of C_3H_6/CO, and CO/CO_2 are given in Table 2. The ratio of C_3H_6/CO_2 can be derived by

Table 2
Catalytic performance of $Mn_{0.18}V_{0.3}Cr_{0.23}W_{0.26}O_x$–$Al_2O_3$ in the ODP reaction at different temperatures and partial pressures of oxygen

$p(C_3H_8)$ (kPa)	$p(O_2)$ (kPa)	τ (kg s m^{-3})	T (K)	$X(C_3H_8)$ (%)	$S(C_3H_8)$ (%)	CO/CO_2[a]	C_3H_6/CO[a]
0.40	0.20	80	723	2.2	74	1.4	1.7
0.40	0.09	200	723	2.8	77	1.5	1.9
0.40	0.04	200	723	2.5	78	1.1	2.3
0.40	0.20	80	773	5.7	70	1.7	1.3
0.40	0.09	200	773	6.8	71	1.5	1.4
0.40	0.04	200	773	5.4	73	0.9	1.9

[a] The ratios were calculated from mole fractions.

multiplying the latter two ratios. At all temperatures, propene selectivity increases slightly with a decrease in oxygen partial pressure. Moreover, the ratio of CO/CO_2 decreases with a decrease in oxygen partial pressures. This means that reaction pathways of CO and CO_2 formation differently depend upon oxygen partial pressure. As a result the ratio of C_3H_6/CO increases but the ratio of C_3H_6/CO_2 slightly decreases with a decrease in oxygen partial pressure. Based on these results, it can be concluded that the reaction pathways of C_3H_6 and CO_2 formation have a similar reaction order with respect to oxygen partial pressure.

The influence of oxygen initial concentration on C_3H_6 selectivity and on the ratio of CO/CO_2 is shown in Fig. 6; the ratio of C_3H_8/O_2 was kept constant and corresponded to 2. For all these data, the degree of propane conversion was ca. 2%. It is clear that propene selectivity increases with a decrease in partial pressures of oxygen. It has to be mentioned again, that in these experiments the inlet ratio of C_3H_8/O_2 was always constant. Taking into account experimental findings from Table 2, it can be assumed that oxygen partial pressure has a stronger effect on propene selectivity as compared to propane partial pressure. Moreover, the CO/CO_2 ratio decreases with a decrease in partial pressure of oxygen. The selectivity to CO drops strongly as compared to the selectivity to CO_2, when oxygen partial pressure decreases. This is in a good agreement with our data on the role of adsorbed oxygen species in CO and CO_2 formation under transient conditions (Section 3.2). Adsorbed oxygen species participate obviously more actively in CO formation than in CO_2 formation (Table 1). It can be assumed that the concentration of adsorbed oxygen species decreases with a decrease in oxygen partial pressure resulting in a decrease in CO formation.

For deriving additional insights into consecutive propene transformations, the ODP reaction was performed with the addition of propene to the ODP reaction feed. In the temperature range from 673 to 723 K, propane conversion decreased slightly, on the addition of propene to the feed mixture. This means that propane and propene compete for the same active catalyst sites, i.e., lattice oxygen species. The product ratios of CO/C_3H_6 and CO_2/C_3H_6 increased with an increase in propene concentration indicating oxidation of propene to CO_x (Fig. 7). However, the ratio of CO/CO_2 decreases linearly with an increase in concentration of propene added. Based on this data, it can be concluded that CO_2 formation is increased in the presence of gas-phase propene.

The effect of temperature on selectivity in the ODP reaction is shown in Fig. 8. Product selectivities were acquired at similar degrees of propane conversion (~2%). The selectivity towards propene increases with an increase in temperature. Additionally, reaction temperature has a stronger effect on the ratios of C_3H_6/CO_2 and CO/CO_2 as

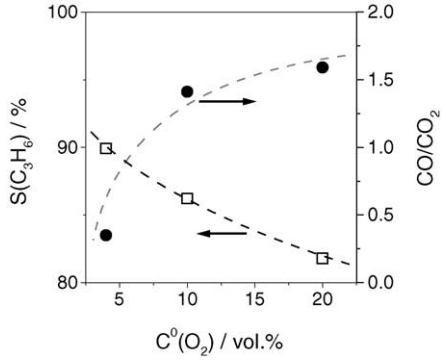

Fig. 6. C_3H_6 selectivity and the CO/CO_2 ratio vs. initial oxygen concentration ($C^0_{O_2}$) at 773 K. The ratio of C_3H_8/O_2 = 2 for all oxygen concentrations.

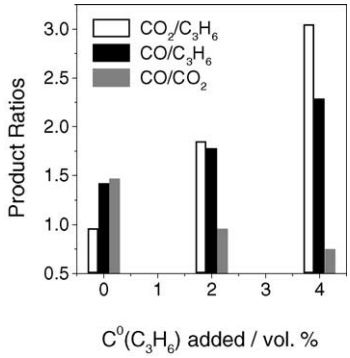

Fig. 7. Influence of the initial concentration of propene ($C^0_{C_3H_6}$) added to the feed (C_3H_8:O_2:N_2 = 20:10:70) on the ratios of C_3H_6/CO, C_3H_6/CO_2 and CO/CO_2 at 773 K.

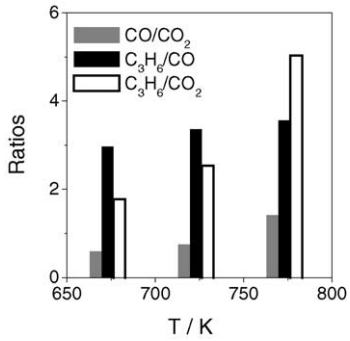

Fig. 8. Effect of temperature on the ratios of C_3H_6/CO, C_3H_6/CO_2 and CO/CO_2 in the ODP reaction (C_3H_8:O_2:N_2 = 20:10:70) over $Mn_{0.18}V_{0.3}Cr_{0.23}W_{0.26}O_x$–$Al_2O_3$ catalyst; propane conversion: ca. 2% at all temperatures.

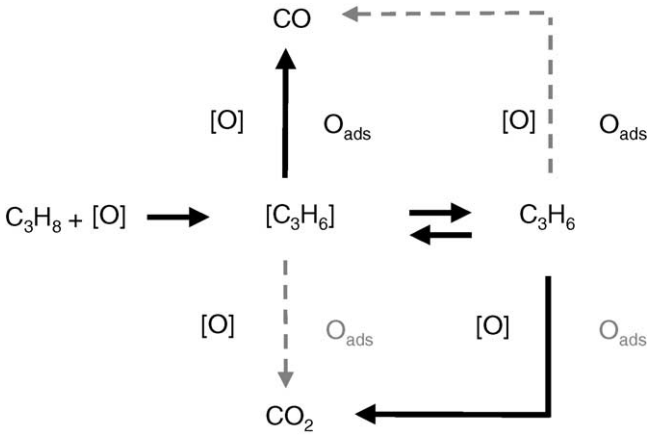

Fig. 9. Suggested reaction scheme of propane oxidation over $Mn_{0.18}V_{0.3}Cr_{0.23}W_{0.26}O_x$–$Al_2O_3$ catalyst. [O] is lattice oxygen, [C_3H_6] is adsorbed propene, and O_{ads} is adsorbed oxygen. Grey arrows and characters are for minor reaction pathways and active species, respectively.

compared to the ratio of C_3H_6/CO (Fig. 8). This indicates that the reaction pathways of CO and C_3H_6 formation have higher activation energies than that of CO_2 formation.

3.4. Reaction network of the ODP reaction

The results of catalyst characterization and catalytic tests are discussed in order to elaborate a mechanistic reaction network of the ODP reaction, which provides insights into the formation of the ODP reaction products under different reaction conditions. With respect to the initial steps of the ODP reaction (O_2 and C_3H_8 activation), a Mars–Van Krevelen type reaction mechanism [31] is suggested taking into account the results of UV–visible and transient studies (Sections 3.1 and 3.2), where lattice oxygen was identified as reactive species for propene and CO_x formation. It is clear that the catalyst can oxidize propane in the absence of gas-phase oxygen. The reduced catalyst is easily reoxidized by gas-phase oxygen. The Mars–Van Krevelen mechanism has been previously discussed for different vanadia [1,5,13,32] and chromia [25] based catalysts. From our results, obviously lattice oxygen of both VO_x and CrO_x aggregates is responsible for propane activation. Molybdenum and tungsten oxides are assumed to be considerably less active under our experimental conditions as has been previously reported [15]. These oxides behave like a support material enabling isolation of active VO_x and CrO_x species, which improves catalytic performance of vanadia and chromia. Similar effects were suggested for the oxidative dehydrogenation of ethane over chromia-based catalysts [25].

CO_x products are formed in the absence of gas-phase oxygen, when propane is pulsed over an oxidized $Mn_{0.18}V_{0.3}Cr_{0.23}W_{0.26}O_x$–$Al_2O_3$ catalyst (Fig. 3). This demonstrates clearly that CO_x formation proceeds also via a Mars–Van Krevelen mechanism with participation of lattice oxygen. The major reaction route of CO and CO_2 formation is the consecutive oxidation of propene, which is a primary product of propane oxidation. Therefore, it can be concluded that propene is activated in competition with propane resulting finally in combustion products. However, it is important to note, that on adding propene to a propane/oxygen mixture, the ratio CO/CO_2 decreases strongly (Fig. 7). This indicates that CO_2 is preferentially formed from gas-phase propene adsorbed on the catalytic surface. In a consistent way, propane and propene compete for lattice oxygen species. This is in contradiction to the study of Zanthoff et al. [14], who suggested that weakly bound adsorbed oxygen species as compared to lattice oxygen are only active for non-selective propane oxidation over a V–MgO_x catalyst. In our case, adsorbed oxygen species were additionally identified to participate mainly in non-selective CO formation as compared to CO_2 formation (Fig. 2 and Table 2). Thus, over a $Mn_{0.18}V_{0.3}Cr_{0.23}W_{0.26}O_x$ on Al_2O_3 catalyst, both adsorbed oxygen species and lattice oxygen take part in CO and CO_2 formation with the latter being the most active one (Table 1 and Fig. 3).

Based on the above results, a simplified scheme for the ODP reaction over the $Mn_{0.18}V_{0.3}Cr_{0.23}W_{0.26}O_x$ on Al_2O_3 catalyst is suggested (Fig. 9). The scheme includes participation of lattice oxygen in propane activation as the primary step of the ODP reaction. Lattice ([O]) and adsorbed oxygen (O_{ads}) species take part additionally in CO_x formation from propene. The main reaction routes and oxygen species are given in black, while minor reaction routes and oxygen species are presented in grey. This reaction scheme considers CO and CO_2 formation via different intermediates. This is in good agreement with experimental data on the dependence of CO and CO_2 formation on O_2, C_3H_8 and C_3H_6 partial pressures (Figs. 6 and 7 and Table 2).

3.5. Optimized conditions for propene formation

The experimental results on the oxidative dehydrogenation of propane show that non-selective consecutive propene

oxidation is the main source of CO_x formation. Direct C_3H_8 oxidation to carbon oxides plays a minor role. From the transient study in the TAP reactor (Section 3.2 and Fig. 3), non-selective reactions are inhibited by a partially reduced catalyst surface. Based on these results, propane oxidation in a periodic mode can be assumed as alternative mode of operation as has been previously suggested for various oxidation reactions [23,33,34] including the oxidative dehydrogenation of propane [35]. In this mode hydrocarbon and air are fed separately and consecutively in the reactor. This concept was put into practice by DuPont for the oxidation of *n*-butane to maleic anhydride [34]. However, for such mode of reactor operation, the catalytic material has to be mechanically stable under reaction conditions offering a high amount of lattice oxygen for the oxidation reaction. Furthermore, the time of catalyst re-oxidation should be matched to that of the reaction. Finally, the near surface concentration of lattice oxygen needs optimisation.

Under conditions of co-feeding oxygen and propane, the non-selective reactions were observed to decrease with an increase in reaction temperature (Fig. 8 and Table 1) and with a decrease in oxygen partial pressure. The increase in selectivity with temperature, however, suggests that there is an optimum temperature and this relationship can be explained by the higher apparent activation energy for propene formation as compared to non-selective consecutive propene oxidation. The influence of oxygen partial pressure is determined by the different reaction orders with respect to oxygen for selective and non-selective reaction routes. In agreement with the above redox mechanism for ODP, a higher concentration of gas-phase oxygen implies a higher rate of its transformation into lattice oxygen, which influences the rate of propane activation and consecutive propene oxidation. The ratio of CO/CO_2 is also influenced by oxygen partial pressure; the higher the oxygen partial pressure the higher is the ratio of CO/CO_2. This is due to participation of adsorbed oxygen species in CO formation as found from the TAP study (Table 1); the concentration of these adsorbed oxygen species depends on oxygen partial pressure.

Based on the above discussion, it is assumed that the selective propane oxidation can be carried out in a co-feed mode at highest possible reaction temperature, at which gas-phase reactions are still insignificant as well as at an optimized C_3H_8/O_2 ratio in order to achieve possible highest selectivity towards propene at the complete oxygen conversion. Previously, Argyle et al. [36] have also concluded that the highest yield of alkene in the oxidative dehydrogenation of ethane and propane is obtained for alumina-supported vanadia catalysts operating at high temperatures that avoid homogeneous reactions. The non-reacted propane is recycled. The efficiency of such type of reactor operation will be determined by the costs for separation of propane and propene at the reactor outlet.

4. Conclusions

The ODP reaction was studied over an optimized catalytic material ($Mn_{0.18}V_{0.3}Cr_{0.23}W_{0.26}O_x$–$Al_2O_3$) by means of kinetic and mechanistic studies under steady-state and transient conditions. The following conclusions were derived:

- A Mars–Van Krevelen mechanism involving lattice oxygen is suggested for both selective and non-selective oxidation steps over $Mn_{0.18}V_{0.3}Cr_{0.23}W_{0.26}O_x$–$Al_2O_3$ as catalytic material. Consecutive non-selective oxidation of propene to CO_x competes with the selective conversion of propane to propene.
- CO and CO_2 are mainly formed via secondary oxidation of propene with participation of lattice oxygen. Additionally, adsorbed oxygen species are active for CO formation. However, they play a minor role under transient conditions.
- The presence of gas-phase propene in the reaction feed favours CO_2 formation over CO formation.
- A partially reduced catalytic surface was found to be more selective for propane dehydrogenation reaction than a fully oxidized one. This is due to the decrease in the near surface concentration of active lattice oxygen by initial interaction with propane or propene and subsequent isolation of active lattice oxygen on the catalyst surface. In turn, the non-selective secondary oxidation of propene to CO_x is inhibited, since for CO_x formation more than one neighbouring lattice oxygen is needed.
- C_3H_6 selectivity is a function of reaction temperature as well as partial pressures of propane and oxygen. The selectivity is improved by an increase in reaction temperature and a decrease in oxygen partial pressure.

Acknowledgement

This work was supported by Deutsche Forschungsgemeinschaft (DFG) in the frame of the priority program (Sonderforschungsbereich 546) ‘‘Structure, dynamics and reactivity of transition metal oxide aggregates’’.

References

[1] E.A. Mamedov, V.C. Corberan, Appl. Catal. A 127 (1995) 1.
[2] F. Cavani, F. Trifiro, Catal. Today 51 (1999) 561.
[3] M. Baerns, G. Grubert, E.V. Kondratenko, D. Linke, U. Rodemerk, Oil Gas-Eur. Mag. 1 (2003) 36.
[4] S. Albonetti, F. Cavani, F. Trifiro, Catal. Rev. Sci. Eng. 38 (1996) 413.
[5] O.V. Buyevskaya, M. Baerns, Catalysis 16 (2002) 155.
[6] J. Le Bars, A. Auroux, M. Forissier, J.C. Vedrine, J. Catal. 162 (1996) 250.
[7] T. Blasco, A. Galli, J.M. Lopez Nieto, F. Trifiro, J. Catal. 169 (1997) 203.
[8] A. Khodakov, B. Olthof, A.T. Bell, E. Iglesia, J. Catal. 181 (1999) 205.

[9] E.V. Kondratenko, M. Baerns, Appl. Catal. A 222 (2001) 133.
[10] G. Centi, E. Giamello, D. Pinelli, F. Trifiro, J. Catal. 130 (1991) 220.
[11] G. Centi, D. Pinelli, F. Trifiro, D. Ghoussoub, M. Guelton, L. Gengembre, J. Catal. 130 (1991) 238.
[12] F. Cavani, F. Trifirò, Catal. Today 36 (1997) 431.
[13] O.V. Buyevskaya, M. Baerns, Catal. Today 42 (1998) 315.
[14] H.W. Zanthoff, S.A. Buchholz, A. Pantazidis, C. Mirodatos, Chem. Eng. Sci. 54 (1999) 4397.
[15] K. Chen, A.T. Bell, E. Iglesia, J. Phys. Chem. 104 (2000) 1292.
[16] K. Chen, A. Khodakov, J. Yang, A.T. Bell, J. Catal. 186 (1999) 325–333.
[17] K. Chen, E. Iglesia, A.T. Bell, J. Catal. 192 (2000) 197–203.
[18] R. Grabowski, J. Sloczyñski, N.M. Grzesik, Appl. Catal. A (2002).
[19] D.B. Creaser, B. Andersson, Appl. Catal. A 141 (1996) 131.
[20] S.L.T. Andersen, Appl. Catal. A 112 (1994) 209.
[21] D. Creaser, B. Anderson, R.R. Hudgins, P.L. Silverston, Can. J. Chem. Eng. (2000) 182.
[22] J.N. Michaels, D.L. Stern, R.K. Grasselli, Catal. Lett. 42 (1996) 139.
[23] D. Creaser, B. Andersson, R.R. Hudgins, P.L. Silveston, Chem. Eng. Sci. 94 (1999) 4437.
[24] O.V. Buyevskaya, A. Brückner, E.V. Kondratenko, D. Wolf, M. Baerns, Catal. Today 67 (2001) 369–378.
[25] G. Grubert, E. Kondratenko, S. Kolf, M. Baerns, P. van Geem, R. Parton, Catal. Today 81 (2003) 337.
[26] A.N. Shigapov, G.W. Graham, R.W. McCabe, H.K. Plummer Jr., Appl. Catal. A 210 (2001) 287.
[27] J.T. Gleaves, G.S. Yablonsky, P. Phanawadee, Y. Schuurman, Appl. Catal. A 160 (1997) 55.
[28] J.T. Gleaves, J.R. Ebner, T.C. Kuechler, Catal. Rev. Sci. Eng. 30 (1988) 49.
[29] G. Centi, S. Perathoner, F. Trifiro, J. Phys. Chem. 96 (1992) 2617.
[30] B.M. Weckhuysen, I.E. Wachs, R.A. Schoonheydt, Chem. Rev. (1996) 3327.
[31] P. Mars, D.W. Van Krevelen, Chem. Eng. Sci. 3 (1954) 41–59.
[32] M.A. Bañares, Catal. Today 51 (1999) 319.
[33] A.C. Jones, J.J. Leonardo, A.J. Sofranko, 4443644 (1984), to Atlantic Richfield Company.
[34] J.J. Lerou, P.L. Mills, Butane oxidation process, in: Precision Process Technology, Kluwer Academic Publishers, Amsterdam, 1993, p. 175.
[35] N. Ballarini, F. Cavani, C. Cortelli, C. Giunchi, P. Nobili, F. Trifirò, R. Catani, U. Cornaro, Catal. Today 78 (2003) 353.
[36] M.D. Argyle, K. Chen, A.T. Bell, E. Iglesia, J. Catal. 208 (2002) 139.